

Published in final edited form as:

*J Pharm Sci.* 2010 May ; 99(5): . doi:10.1002/jps.22003.

## Swellable Microparticles as Carriers for Sustained Pulmonary Drug Delivery

IBRAHIM M. EL-SHERBINY<sup>1,2</sup>, SHAYNA MCGILL<sup>1</sup>, and HUGH D.C. SMYTH<sup>1,3</sup>

<sup>1</sup>Division of Pharmaceutical Sciences, College of Pharmacy, University of New Mexico, Albuquerque, New Mexico 87131

<sup>2</sup>Polymer Laboratory, Faculty of Science, Chemistry Department, Mansoura University, ET-35516 Mansoura, Egypt

<sup>3</sup>Lovelace Respiratory Research Institute, Albuquerque, New Mexico 87108

### Abstract

In this investigation, novel biodegradable physically crosslinked hydrogel micro-particles were developed and evaluated *in vitro* as potential carriers for sustained pulmonary drug delivery. To facilitate sustained release in the lungs, aerosols must first navigate past efficient aerodynamic filtering to penetrate to the deep lung (requires small particle size) where they must then avoid rapid macrophage clearance (enhanced by large particle size). The strategy suggested in this study to solve this problem is to deliver drug-loaded hydrogel microparticles with aerodynamic characteristics allowing them to be respirable when dry but attain large swollen sizes once deposited on moist lung surfaces to reduce macrophage uptake rates. The microparticles are based on PEG graft copolymerized onto chitosan in combination with Pluronic® F-108 and were prepared via cryomilling. The synthesized polymers used in preparation of the microparticles were characterized using FTIR, EA, 2D-XRD, and differential scanning calorimetry (DSC). The microparticles size, morphology, moisture content, and biodegradation rates were investigated. Swelling studies and *in vitro* drug release profiles were determined. An aerosolization study was conducted and macrophage uptake rates were evaluated against controls. The microparticles showed a respirable fraction of approximately 15% when prepared as dry powders. Enzymatic degradation of microparticles started within the first hour and about 7–41% weights were remaining after 240 h. Microparticles showed sustained release up to 10 and 20 days in the presence and absence of lysozyme, respectively. Preliminary macrophage interaction studies indicate that the developed hydrogel microparticles significantly delayed phagocytosis and may have the potential for sustained drug delivery to the lung.

### Keywords

drug delivery; chitosan; PEG; microparticles; pulmonary; lung; inhalation therapy; hydrogels; sustained drug release

### INTRODUCTION

The last few years have witnessed a great interest in studying the delivery of therapeutic molecules administered by pulmonary route for both local and systemic treatments. This great deal of attention is due to the numerous advantages of pulmonary drug delivery over

many other delivery routes. These advantages include the large alveolar surface area suitable for drug absorption, low thickness epithelial barrier, extensive vascularization, and the relatively low enzymatic metabolic activity in addition to the absence of the first-pass effect.<sup>1–3</sup>

However, due to the efficiency of local clearance mechanisms, designing a respirable carrier system with adequate aerodynamic properties that can confer sustained release of drug once deposited in lung is considered one of the major challenges in pulmonary drug delivery.<sup>3,4</sup> Particles, targeted to the deep lung, should be small enough (0.5–5  $\mu\text{m}$  aerodynamic diameters) to pass through the mouth, throat, and conducting airways and reach the deep lung, but not so small ( $<0.5 \mu\text{m}$ ) that they fail to deposit and are exhaled again.<sup>4</sup> Understandably from an evolutionary and pulmonary toxicology perspective, microparticles of these sizes have rapid clearance from lung by alveolar macrophages. Increasing microparticle size has been shown to reduce macrophage phagocytosis;<sup>5,6</sup> however, increasing particle size is impractical for pulmonary drug delivery purposes due to the efficient filtering role performed by the upper airways. Therefore, development of swellable microparticles that have respirable aerodynamic sizes when dry but, upon deposition in the lung, attain larger geometric sizes via controlled swelling to avoid macrophage clearance represents a very promising strategy. In these studies, we designed respirable hydrogel microparticles based on chitosan (Cs), poly(ethylene glycol) (PEG), and Pluronic<sup>®</sup> polymer systems.

Cs [a (1  $\rightarrow$  4)-2-amino-2-deoxy- $\beta$ -D-glucan] is a cationic biopolymer obtained through alkaline *N*-deacetylation of natural chitin. Cs has numerous desirable properties such as biodegradability, non-toxicity, and biocompatibility.<sup>7–9</sup> It has been reported also that Cs has many advantageous characteristics for improving drug absorption, such as protection of the drug against enzymatic degradation<sup>10</sup> and absorption-enhancing effects in both GI tract<sup>11,12</sup> and nasal mucosa.<sup>13,14</sup> Recently, it has been confirmed also that Cs has a significant drug absorption-enhancing effect in the pulmonary tissues.<sup>15</sup> It was suggested that the absorption-enhancing mechanism of Cs in lung tissues might be due to transient opening of the intercellular tight junction of the lung epithelium, which is the same mechanism already reported for intestinal and nasal mucus membranes.<sup>15</sup> Moreover, the reactive amino groups in the backbone of Cs make it possible to chemically conjugate various molecules, which may improve performance of the delivery system.<sup>16,17</sup> These characteristics make Cs an ideal candidate in the preparation of hydrogel carriers for controlled drug release.<sup>16–18</sup>

PEG is a highly water-soluble polymer. Due to the high hydrophilicity, lack of toxicity and biocompatibility of PEG, grafting of it onto Cs is considered to be a convenient route to synthesize drug carriers with desirable features.<sup>19</sup> In addition, it has been widely shown that PEG coating on micro and nanoparticles leads to decreased macrophage engulfment.<sup>5</sup> Of different polymeric carriers based on Cs derivatives with improved hydrophilicity, nanosized hydrogel particles based on PEG graft copolymerized onto Cs have received recently a growing interest as novel potential carriers for drugs.<sup>20–26</sup>

Pluronics<sup>®</sup> is a class of biocompatible water-soluble triblock copolymers (also known as “poloxamers”). These block copolymers consist of hydrophilic poly (ethylene oxide) (PEO) and hydrophobic poly(propylene oxide) (PPO) blocks arranged in A–B–A triblock structure: PEO-*b*-PPO-*b*-PEO.<sup>27</sup> Pluronics<sup>®</sup> have found widespread use for many biomedical applications. These include cell encapsulation<sup>28</sup> and coatings for medical devices.<sup>29</sup> Also, Pluronics<sup>®</sup> have been used in drug delivery systems such as hydrogels and micelles<sup>30,31</sup> that are FDA approved. The main feature of these polymers is their amphiphilic character, which enables them to display surfactant properties including ability to interact with hydrophobic surfaces and biological membranes. In addition, this amphiphilic nature is a reason for

success of Pluronics<sup>®</sup> in drug delivery as it allows the solubilization of hydrophobic drugs in an aqueous environment and increases drug stability and also improves the drug pharmacokinetics and biodistribution.

In this study, novel biodegradable physically cross-linked (amphiphilic interactions) hydrogel micro-particles were developed and evaluated *in vitro* as potential carriers that can confer pulmonary sustained drug delivery. These hydrogel microparticles were prepared to show desired respirable aerodynamic size when dry but large swollen size when deposited in the lung to avoid macrophage clearance. The micro-particles are based on PEG graft copolymerized onto Cs in combination with Pluronic<sup>®</sup> F-108 and were prepared in mild conditions via cryomilling. To the best of our knowledge, these are the first studies to investigate swellable microparticles for pulmonary drug delivery.

## MATERIALS AND METHODS

### Materials

Monomethoxypoly(ethylene glycol) (m-PEG, Mn 5000 Da), Cs (medium MW, % *N*-deacetylation; about 76.4%, as determined by elemental analysis), succinic anhydride and 1-hydroxybenzotriazole (HOBt) were purchased from Aldrich, St. Louis, MO. Pluronic<sup>®</sup> F-108 Pastille was obtained from BASF, Chattanooga, TN Corporation. 1-ethyl-3-(3-dimethylaminopropyl) carbodiimide hydrochloride (EDC·HCL) was purchased from Fluka Chemical Corp (Milwaukee, WI). 4-Dimethylaminopyridine (DMAP) was provided by Sigma, St. Louis, MO. Phthalic anhydride, sodium fluorescein (SF), triethyl amine, hydrazine monohydrate, dioxane, and dimethyl formamide (DMF) were obtained from Sigma–Aldrich, St. Louis, MO, SIAL. Lactose excipient (Respitose<sup>®</sup> ML001 was obtained from DMV-Fonterra Excipients (Goch, Germany). Phosphate-buffered saline (PBS, pH 7.4) and all other reagents were of analytical grade and used as received.

### Methods

**Synthesis of PEG-Cs Graft Copolymer**—The copolymer of m-PEG macromer grafted onto Cs was prepared by a modified method to that reported by Yoksan et al.<sup>32</sup> and Yoksan and Chirachanchai.<sup>33</sup> The synthesis sequence was as follows.

Firstly, the free NH<sub>2</sub> groups of Cs were protected via *N*-phthaloylation. In brief, 10 g Cs was reacted with phthalic anhydride (44.8 g, 5 mol equivalent to pyranose rings) in DMF (200 mL) at 130°C under nitrogen atmosphere for 8 h. The product of *N*-phthaloyl Cs (NPHCs) was then collected by filtration after precipitation in cold water, washed with methanol, and then dried under vacuum.

m-PEG was converted into m-PEG-COOH by reacting with succinic anhydride. Briefly, m-PEG (100 g, 20 mmol), succinic anhydride (2.4 g, 24 mmol), DMAP (2.44 g, 20 mmol), and triethylamine (2.02 g, 20 mmol) were dissolved in dry dioxane (350 mL). The reaction mixture was stirred at room temperature for 48 h under nitrogen atmosphere. Dioxane was evaporated under vacuum and the residue was taken up in CCl<sub>4</sub>, filtered, and precipitated by diethyl ether.

Grafting of m-PEG-COOH onto NPHCs was then performed by stirring m-PEG-COOH (37.9 g) with NPHCs (5.0 g, 0.4 mol equivalent to m-PEG-COOH) in 75 mL of DMF. HOBt (3.4 g, 3 mol equivalent to m-PEG-COOH) was then added and the stirring was continued at room temperature until obtaining a clear solution. Then, EDC·HCl (4.25 g, 3 mol equivalent to m-PEG-COOH) was added and the reaction was stirred overnight at room temperature. The reaction mixture was then dialyzed against distilled water and washed with ethanol to remove unreacted macromer.

Finally, the PEG-g-Cs copolymer was synthesized by deprotection of the  $\text{NH}_2$  groups of the PEG-g-NPHCs produced in the previous step using hydrazine monohydrate. Typically, PEG-g-NPHCs (4.0 g) was heated to  $100^\circ\text{C}$  with stirring under nitrogen in 15 mL of DMF. Then hydrazine monohydrate (20 mL) was added and the reaction was continued for 2 h. The mixture was then dialyzed against distilled water and ethanol and then dried under vacuum.

**N-phthaloyl Cs:** FTIR ( $\nu_{\text{max}}$ ,  $\text{cm}^{-1}$ ), 3281 (OH stretching and NH bending), 2961 (C–H stretching), 1775 and 1698 (C–O anhydride), 1395 (C–C, phthaloyl), 1058 (C–O, pyranose), and 732 (aromatic ring of phthaloyl). EA,  $(\text{C}_8\text{H}_{13}\text{NO}_5)_{0.2363}(\text{C}_6\text{H}_{11}\text{NO}_4)_{0.016}(\text{C}_{14}\text{H}_{13}\text{NO}_6)_{0.747}$ , anal. calculated (DS = 0.98) (%): C, 55.74; H, 4.84; and N, 5.23, found (%): C, 60.31; H, 4.83; and N, 4.92.

**m-PEG-COOH (yield:  $\approx 98\%$ ):** FTIR ( $\nu_{\text{max}}$ ,  $\text{cm}^{-1}$ ) 3496 (OH stretching), 2882 (C–H stretching), 1733 (C–O of carboxylic group), and 1102 (C–O–C stretching); EA  $(\text{C}_{231}\text{H}_{460}\text{O}_{117})$ , anal. calculated (%): C, 54.35 and H, 9.02, found (%): C, 56.8 and H, 9.19.

**PEG-g-NPHCs (5.47 g):** FTIR ( $\nu_{\text{max}}$ ,  $\text{cm}^{-1}$ ) 3423 (OH stretching and NH bending), 2879 (C–H stretching), 1736 (C–O ester and anhydride), 1703 (C–O anhydride), 1096 (C–O–C stretching), and 723 (aromatic ring of phthaloyl). EA, found (%): C, 56.16; H, 4.69; and N, 5.15.

**PEG-g-Cs:** FTIR ( $\nu_{\text{max}}$ ,  $\text{cm}^{-1}$ ) 3312 (OH stretching, NH bending, and intermolecular H-bonding), 2879 (C–H stretching), 1708 (C–O ester), and 1096 (C–O–C stretching). EA, found (%): C, 40.46; H, 4.71; and N, 14.44.

**Characterization**—The elemental analysis for Cs, NPHCs, m-PEG-COOH, PEG-g-NPHCs, and PEG-g-Cs copolymers was performed with Costech ECS4010 Elemental Analyzer coupled to a Thermo-Finnigan Delta Plus Isotope Ratio Mass Spectrometer. Also, the prepared polymers were characterized by FTIR (Nicolet 6700 FTIR spectrometer). Differential scanning calorimetry (DSC) of the synthesized polymers was performed using DSC 2920 (Modulated DSC, TA Instruments, Woodland, CA) in a nitrogen atmosphere from  $-40^\circ\text{C}$  to  $400^\circ\text{C}$  at a heating rate of  $10^\circ\text{C}/\text{min}$ . The samples (10–12 mg) were weighed into aluminum sample pans and sealed. An empty aluminum pan of approximately equal weight was used as a reference. All peaks were determined and the areas were converted into enthalpy values.

**Preparation of Microparticles**—The hydrogel microparticles were prepared via cryo-milling of polymer films. In a typical procedure, solutions of PEG-g-Cs and Pluronic<sup>®</sup>F-108 (1%, w/w) were prepared by dissolving the predetermined weight of each polymer in 0.1 M acetic acid and distilled water, respectively, with stirring at room temperature. The polymer solutions were then filtered through glass-wool and allowed to degas. The polymer films were obtained by casting 50 mL of polymers mixtures of different compositions (see Tab. 1) onto polystyrene Petri dishes and allowing the solvent to evaporate at room temperature. The dry films were then collected, washed several times with 0.1 M NaOH to neutralize the acetate salt and then with distilled water, and dried at room temperature. The air-dried films were then cut into small pieces and 150 mg of each were cryomilled using a 5-mL stainless steel milling vial containing a stainless steel ball. Cryomilling process was carried out by immersing the sealed vial in liquid nitrogen for 5 min followed by 15 min of milling in liquid nitrogen then vigorous milling out of liquid nitrogen for extra 5 min. The micronized particles were stored in a desiccator until further investigation.

**Microparticles Size Determination**—The size of the developed hydrogel microparticles and particle size distribution were determined using laser diffraction equipment (SYMPATEC, Sympatec GmbH, System Partikel-Technik (Clausthal-Zellerfeld Germany) with a He–Ne laser beam 5 mW max at 632.8 nm) using WINDOX 5.1.2 software. The measurements were carried out in the range 0.5–175  $\mu\text{m}$  for the suspension of the hydrogel microparticles in acetone. Volume median diameters (VMD) were calculated from the particle size distribution curves. VMD ( $D_{50}$ ) is the particle diameter at which half the particles volume is contributed by particles larger than the VMD and half by particles smaller than the VMD. For estimation of aerodynamic diameters of the microparticles, particle densities were approximated from tapped density experiments since aerodynamic diameters are related to density and VMD as shown in the following relationship:

$$d_a = d_g \left( \frac{\rho_p}{\rho_0 \chi} \right)^{1/2} \quad (1)$$

where  $d_a$  is the particle aerodynamic diameter ( $\mu\text{m}$ ),  $d_g$  is the geometric diameter (VMD,  $\mu\text{m}$ ),  $\rho_p$  is the particle density ( $\text{g}/\text{cm}^3$ ),  $\rho_0$  is the standard density ( $1 \text{ g}/\text{cm}^3$ ), and  $\chi$  is the dynamic shape factor.

Also, microparticle size (sieve and Feret's diameters) was determined directly using optical microscopy (Olympus IX-70, Osakashi, Osaka, Japan) with the aid of ImageJ software. Both the sieve and Feret's diameters were determined as the mean values of 100 microparticles measurement ( $n = 100$ ).

**In Vitro Aerosolization Study**—A Twin Stage Liquid Impinger (TSI, Apparatus A, British Pharmacopoeia, 2007) was used to determine the emitted fraction (EF) and respirable fraction (RF) of the microparticle powders. In a typical procedure, a size 3CS capsule (CapsuGel) was loaded with 20–30 mg of powder (10% SF-loaded hydrogel micro-particles with 90% lactose mixed for 30 min using Turbula® Mixer). The capsule was placed in a handheld, dry-powder, breath-activated inhaler device (Aerolizer®, Novartis, New York, NY). The capsule was punctured prior to inhalation and a pump was actuated to simulate an inspiration (air flow rate of 60 L/min for duration of 10 s). Three capsules were emptied sequentially for each run. The total powder emitted from these three capsules was deposited on different stages of the impinger, mouth-throat, stages 1 and 2. Stages 1 and 2 contain 7 and 30 mL, respectively, of sodium acetate buffer, pH 3.4, as collecting solvent and the powder deposited in mouth-throat region was collected in 5 mL of same buffer. The EF that corresponding the percent of total loaded powder mass exiting the capsules was determined gravimetrically and can be expressed as

$$\text{EF}\% = \left( \frac{m_f - m_e}{m_p} \right) \times 100 \quad (2)$$

where  $m_f$  and  $m_e$  are the weights of the capsule before and after simulating the inhalation and  $m_p$  is the initial weight of the powder. The contents of drug-loaded powder on each stage (mouth-throat, stages 1 and 2) were determined by measuring the absorbance at  $\lambda_{\text{max}}$  of 430 nm using Infinite M 200 fluorophotometer (TECAN San Jose, CA) with the aid of a calibration curve. The ratio of the weight deposited on stage 2 divided by the weight of the powder initially loaded in the capsules is called the RF and is expressed in percent.

**Scanning Electron Microscopy Analysis**—The morphology of the prepared hydrogel microparticles was assessed by scanning electron microscope (SEM; Hitachi S-800 field

emission SEM with a Robinson backscatter detector and with a Hitachi PCI system for digital image capture). Dry microparticles were mounted on aluminum stubs with double-sided conducting carbon tapes and coated with a 50:50 mixture of gold and palladium to minimize surface charging. The sample was scanned at an accelerating voltage of 20 kV.

**Determination of Moisture Content**—The moisture contents (%) of the microparticles were estimated using HR83 Halogen Moisture Analyzer (Mettler-Toledo GmbH, Greifensee, Switzerland). The samples weights were in the range of 100–120 mg and the applied drying temperature was 120°C for 2 min. The moisture content was obtained as a weight loss % and calculated as the average  $\pm$  SD from three independent measurements.

**Swelling Study of Drug-Loaded Microparticles**—The swelling patterns of the hydrogel microparticles loaded with SF, as a model drug, were determined by weighing a certain amount of microparticles (about 20 mg) in an Eppendorf tube and incubating in 1.0 mL of PBS (pH 7.4) in a shaking (150 rpm) water bath at 37°C. At predetermined intervals, the samples were centrifuged at 5000 rpm for 2 min and the supernatants were removed. Then, the weights of the swollen microparticles were determined. The percent swelling was calculated by the following equation:

$$\text{Swelling \%} = \left( \frac{W_t}{W_0} \right) \times 100 \quad (3)$$

where  $W_0$  is the initial weight and  $W_t$  is the final weight of the microparticles at time  $t$ . The swelling data points represent mean  $\pm$  SD from three independent experiments. Also, the swelling values attained by the developed microparticles in PBS (pH 7.4) at the beginning was studied by determination of the increase in VMD ( $\mu\text{m}$ ) of some swelled SF-loaded microparticles using laser diffraction.

**In Vitro Biodegradation Study**—An *in vitro* biodegradation study of the microparticles was carried out in the presence of lysozyme.<sup>34</sup> Typically, lysozyme was dissolved in PBS (pH 7.4) to prepare a solution with a concentration of 2 mg/mL as described by Nsereko and Amiji<sup>34</sup> and Hirano et al.<sup>35</sup> Predetermined weights of microparticles (10–15 mg) were transferred to Eppendorf tubes and incubated in 1.0 mL of lysozyme solution in a shaking (150 rpm) water bath at 37°C for 1 h until the equilibrium swelling of these microparticles almost attained. Then, the samples were centrifuged at 14,500 rpm for 3 min and the supernatant was removed. The weights of the swollen microparticles ( $W_0$ ) were determined. Then 1 mL of fresh lysozyme solution was added to the swollen microparticles. At certain intervals starting from determination of  $W_0$ , the steps of centrifugation and weighing were repeated and the final weights ( $W_t$ ) of microparticles at these intervals were determined. The percent weight remaining of the samples due to enzymatic degradation were determined according to the following equation:

$$\text{Remaining weight \%} = 100 - \left[ \left( \frac{W_0 - W_t}{W_0} \right) \times 100 \right] \quad (4)$$

where  $W_0$  is the weight of sample after 1 h swelling in lysozyme solution and  $W_t$  is the weight of the sample after incubation with lysozyme for a given time  $t$ .

#### **Entrapment of a Model Drug and Determination of Drug Uploading Efficiency**

—Hydrogel microparticles loaded with 0.2% (w/w) SF, as a model for hydrophilic drugs, were prepared in the same manner as described earlier for preparation of drug-free microparticles with the addition of the SF to the solution of polymer mixture before casting. The resulting SF-loaded microparticles were stored in a desiccator at dark until use. The

distribution of the model drug SF within the microparticles was examined by fluorescence microscopy. Dry microparticles were dispersed on glass cover slips and representative fluorescence images were taken using Olympus IX-70 microscope with MagnaFire 2.1 software.

For the determination of drug uploading efficiency, the dried plain and SF-loaded hydrogel microparticles were dissolved in sodium acetate buffer, pH 3.4, to make about 20 mg/mL solutions. The buffer solution has been prepared based on the British Pharmacopoeia 2007 via mixing 5 volumes of 0.1 M sodium acetate with 95 volumes of 0.1 M acetic acid. The absorbance of solutions was measured by UV–Vis spectrophotometry at 434 nm (Beckman Coulter DU® 800 UV–Vis spectrophotometer, Fullerton, CA). Using a standard curve of SF in sodium acetate buffer (pH 3.4) versus absorbance, the amount of SF per gram polymer microparticles was then calculated. The solution of plain microparticles was used as absorbance background control. It has been found in prior studies that there is no absorbance interference from the plain microparticles under the same conditions. The mean values for three replicate determinations and their mean  $\pm$  SD values were reported. The entrapment efficiency (EE%) of the model drug SF was calculated as follows:

$$EE\% = \left( \frac{m_r}{m_i} \right) \times 100 \quad (5)$$

where  $m_i$  and  $m_r$  are the amounts (mg) of the SF initially uploaded and remained in the microparticles, respectively.

**In Vitro Release Studies**—The *in vitro* release profiles of the model drug were determined by weighing a certain amount (15–20 mg) of SF-loaded microparticles in 3 mL vials containing 2 mL of PBS, pH 7.4. Then, all samples were maintained at 37°C with shaking (100 rpm). At predetermined intervals, 500  $\mu$ L of aliquots was withdrawn and analyzed by fluorescence spectrophotometry (Infinite M 200 fluorophotometer, TECAN, i-control 1.5 software) at excitation and emission wavelengths of 495 and 520 nm, respectively, using Nunclon 96 flat bottom black polystyrol LumiNunc plates. The release profiles were also determined by same procedure in PBS, pH 7.4, containing 2 mg/mL of lysozyme. The withdrawn sample was replaced with an equal volume of fresh medium to keep the volume of the release medium constant. It has been found in prior studies that there is no absorbance interference from the plain microparticles under the experimental conditions. The amounts of SF released (mg) from microparticles were then calculated using a standard curve of SF. The SF release was calculated in terms of cumulative release (% w/w) relative to the initial entrapped weight of SF in the microparticles. The data points represent mean  $\pm$  SD from three independent experiments.

**Microparticles Uptake by Macrophages**—Raw 264.7 macrophages (American Type Culture Collection TIB-71, Manassass, VA) were seeded at  $5 \times 10^4$  cells/well into a 24-well plate (Falcon 353047 Multiwell; Becton Dickinson, Franklin Lakes, NJ) containing Dulbecco's modified Eagle medium (DMEM; Invitrogen, Grand Island, NY). After 24 h incubation, DMEM was removed and the cells were washed with PBS (pH 7.4). Then, 25  $\mu$ L of DMEM containing 1  $\mu$ m polystyrene beads, as a control (Fluospheres fluorescent (505/515) F8823; Invitrogen, Eugene, OR), A1 or A3 was added to the labeled wells.<sup>36</sup> The microparticles (polystyrene beads, A1 or A3) were added at desired concentrations so that equal masses of each particle type were incubated with the cells ( $2 \times 10^3$  1  $\mu$ m polystyrene beads/cell and 10  $\mu$ m A1 or A3/cell). One row of wells was left as a cell control that did not contain any particles. After each time point (15 min, 30 min, 1 h, 15 h, and 24 h) media were removed and the cells were washed two times with PBS, fixed with 0.5 mL of 4% PFA solution for 10 min, and then washed with PBS to remove any residual PFA. Wells were

then imaged using an inverted Olympus IX70 microscope at 4× and 10× magnification. Particle uptake was quantified using image analysis of low magnification (to capture as many particles in each field of view) micrographs of each experimental group (ImageJ, NIH).

## RESULTS AND DISCUSSION

### Preparation and Characterization of PEG-g-Cs Copolymer

Biocompatible and biodegradable PEG-g-Cs copolymer was synthesized through a modified method.<sup>32,33</sup> The systematic sequence of the copolymer synthesis is illustrated in Scheme 1 and it started with conversion of m-PEG into carboxyl-capped m-PEG precursor (m-PEG-COOH) upon reaction with succinic anhydride. The m-PEG-COOH was obtained in a good yield (98%) and was characterized using FTIR and EA. The NH<sub>2</sub> groups of Cs were protected via phthaloylation process upon reaction with phthalic anhydride in DMF to produce NPHCs. The synthesis of NPHCs was confirmed by FTIR through appearance of bands at 1395 and 732 cm<sup>-1</sup> which correspond to C–C and the aromatic ring of the phthaloyl group, respectively. The degree of substitution (DS) of phthaloyl group was estimated to be 0.979 using elemental analysis. Then grafting of m-PEG-COOH onto NPHCs was carried out in DMF (grafting %; 9.34%). The PEG-g-Cs copolymer (grafting; 31.8%) was then obtained by deprotection of NH<sub>2</sub> groups of PEG-g-NPHCs copolymer using N<sub>2</sub>H<sub>4</sub>·H<sub>2</sub>O. The synthesis of PEG-g-Cs was confirmed using EA and FTIR. The synthesis sequence of the graft copolymer is illustrated in Scheme 1.

Figure 1 depicts the DSC curves for Cs and PEG-g-Cs copolymer. In case of Cs thermogram (Fig. 1a), it shows an endothermic peak started at 90°C, which can be ascribed to the loss of bound water. Cs shows also an exothermic peak at 312°C which may be related to the decomposition of glucosamine units.<sup>37,38</sup> The thermogram of PEG-g-Cs (Fig. 1b) shows an endothermic peak at 55°C which can be attributed to the melting of the grafted PEG side chains. Also, an endotherm was observed at 119°C which may be due to the loss of bound water. The exothermic peaks appeared at 261 and 310°C may be attributed to the crystallization and decomposition of the graft copolymer, respectively.

### Preparation of Hydrogel Microparticles

The graft copolymer, PEG-g-Cs (31.8% grafting), synthesized in this study was used to prepare respirable hydrogel microparticles as novel biodegradable carriers for pulmonary sustained drug delivery. As shown in Table 1, the developed hydrogel microparticles are based on either PEG-g-Cs alone or its combination with Pluronic® F-108. The microparticles were prepared in mild conditions via cryomilling of dried polymer thin films in the presence of liquid nitrogen. These developed microparticles are physically crosslinked hydrogels formed via the intermolecular amphiphilic interactions between the copolymer and Pluronic® chains and/or the intramolecular amphiphilic interactions between the copolymer chains. A schematic representation of the hydrogel microparticles is illustrated in Scheme 2.

### Microparticles Size

Figures 2 and 3 showed that most of the micro-particles developed in this study are in the form of irregular plates with some others of rounded shape. The platelet shapes of microparticles may be attributed to their initial form as thin films prior to cryomilling.

Designing of appropriate inhaled carrier systems with adequate aerodynamic characteristics for pulmonary drug delivery is critical. Carrier particles should be small enough to reach the deep lung but not so small that they fail to deposit and are exhaled again. The average size

of microparticles can be estimated by determination of their diameters. There are several types of diameters depending on the way of their determination. VMD derived from laser diffraction sizing is shown in Figure 4 and Table 2. The VMD of the developed microparticles is in the range between  $11.13 \pm 0.45$  and  $13.73 \pm 0.07$   $\mu\text{m}$ . It was found that increasing the percent of Pluronic® F-108 tends to decrease the size. For example, the average VMD of A1 (0% Pluronic), A2 (10% Pluronic), and A3 (40% Pluronic) are  $13.73 \pm 0.07$ ,  $12.06 \pm 0.13$ , and  $11.13 \pm 0.23$   $\mu\text{m}$ , respectively. This may be attributed to increasing the brittleness of the dried hydrogel films with increasing the Pluronic percent, which would lead to more efficient micronization during the cryomilling process.

Sieve and Feret's diameters are two other methods that estimate the particle size for dry powder inhalation purposes. These were estimated using optical microscopy with aid of "ImageJ" software, (NIH). Feret's diameter is the measured distance between two tangents on opposite sides of the particle (Fig. 5a). Inner (sieve) diameter, as illustrated in Figure 5b, is the diameter of the maximum inscribed circle (the maximum circle lying completely inside the particle).<sup>39</sup> The sphere having this sieve diameter passes through the same sieve as the particle itself. As shown in Table 2, the microparticles developed in this study have sieve and Feret's diameters in the range of  $10.96$ – $12.78$   $\mu\text{m}$  and  $16.67$ – $21.81$   $\mu\text{m}$ , respectively. Remarkably, volume diameters and sieve diameters yielded similar results despite the considerable differences in their measurement principles.

### ***In Vitro* Aerosolization Study**

The aerodynamic characteristics of the developed hydrogel microparticles were evaluated using a dry-powder, breath-activated inhaler device (Aerolizer®, Novartis). Powder aerosolization properties were tested using a TSI. Three capsules were aerosolized sequentially from the dry powder inhaler to the TSI. The EFs of the three developed microparticles formulations (A1, A2, and A3) were in the range  $96 \pm 1.8$  to  $98 \pm 0.9$  (Tab. 2). Figure 6 shows the aerodynamic evaluation of the microparticles. As noted from the figure, the RFs (fraction of the particles  $<6.4$   $\mu\text{m}$  aerodynamic diameter) for the investigated microparticles A1, A2, and A3 were  $15.24 \pm 8.46$ ,  $14.85 \pm 0.87$ , and  $15.07 \pm 0.58$ , respectively. These RF values represent the fractions of the dry powder that may deposit in the lung, and the magnitude of these values is similar to the performance of currently marketed inhaler devices.<sup>40</sup> The hydrogel microparticles A1, A2, and A3 showed total deposited doses of 81.04%, 92.13%, and 77.24%.

As the aerosolization performance and lung deposition efficiencies are determined by aerodynamic diameters, the density of the hydrogel micro-particles was also determined. Aerodynamic diameter is related to geometric diameter through the relationship shown in Eq. (1). Nonspherical high aspect ratio particles and low-density materials reduce the aerodynamic diameter relative to geometric size.<sup>41</sup> As shown in Table 2, the bulk densities of the microparticles are relatively low (about  $0.7$   $\text{g}/\text{cm}^3$ ). Also, SEM images showed high aspect ratio particles. Therefore, aerodynamic diameters of the microparticles are likely to be significantly less than  $10$ – $12$   $\mu\text{m}$  (geometric sizes). This tends to explain the relatively high respirability (RF values) of the particles as demonstrated in the aerosol dispersion study.

### **Scanning Electron Microscopy and Moisture Content of Microparticles**

The morphology of the microparticles is shown in Figure 2. Some of the microparticles are in form of elongated plates while some others are crystalline rough discs. The surface morphology of some of the developed microparticles (Fig. 2c) shows that they have a relatively rough surface.

As noted from the results of moisture contents (%) of drug-free and drug-loaded microparticles (Tab. 1), the microparticles, in general, have relatively low percents of moisture. These low moisture contents are important for long-term stability and avoiding drug degradation. Moreover, low moisture contents reduce the density and consequently improve the aerodynamic performance of the microparticles during inhalation.

### Swelling Characteristics

Figure 7 shows the swelling profiles of drug-loaded microparticles. The SF-loaded (0.2%, w/w) hydrogel microparticles have attained a swelling pattern similar to that found for drug-free microparticles (swelling results of drug-free microparticles will be represented elsewhere, I.M. El-Sherbiny and H.D.C. Smyth, unpublished results). However, the SF-loaded microparticles showed a faster initial rate of swelling, within the first 30 min, and also attained higher values of swelling at equilibrium as compared to the drug-free microparticles. For instance, the SF-loaded A1, A2, and A3 microparticles (Fig. 7) attained swelling values of  $1318 \pm 110\%$ ,  $1101 \pm 22\%$ , and  $1308 \pm 11.6\%$  after 6 h whereas the swelling values attained after 6 h for the corresponding drug-free microparticles were  $1110 \pm 81\%$ ,  $1055 \pm 356\%$ , and  $784 \pm 84\%$ , respectively. This increase in % swelling upon loading SF as a model drug may be attributed to both the expected higher hydrophilicity and small size of the uploaded SF molecules. These two characteristics may facilitate the increased transport of the swelling fluid into the partially swollen hydrogel microparticles. Also, as appeared from Figure 7, the microparticles formulations containing Pluronic® (A2 and A3) showed reduced values of swelling as compared to A1. This effect of Pluronic® content onto swelling values of microparticles can be attributed to the increase in the crosslinking due to the intermolecular amphiphilic interactions between the PEG-g-NPHCs copolymer and Pluronic® chains. The fast swelling attained by the developed microparticles at the beginning was also confirmed by the determination of the VMD ( $\mu\text{m}$ ) of some swelled SF-loaded microparticles as shown in Figure 8.

### In Vitro Biodegradation of Microparticles

An *in vitro* biodegradation study of the developed hydrogel microparticles was carried out in the presence of lysozyme. Lysozyme is abundantly present in a number of human secretions, such as tears, saliva, and mucus including the airways. The remaining weight (%) of microparticles as a function of time was determined and taken as a measure of the enzymatic degradation. Figure 9 shows the enzymatic degradation profiles of the microparticles in PBS (pH 7.4) in the presence of lysozyme. As shown in the figure, the enzymatic degradation of almost all the microparticles formulations started to occur within the first 60 min. The microparticles with high content (40%) of Pluronic® (A3) showed a lower degradation extent (higher values of remaining weight %) than microparticles of lower content (10%) of Pluronic® (A2). For instance, after 240 h, only 7% of A2 weights were remaining while the percent of weight remaining of A3 was almost 41%. This effect of Pluronic® content onto biodegradation rate of microparticles can be returned to the increase in the crosslinking extent upon increasing the Pluronic® percent. This increase in crosslinking slows down the diffusion of enzyme through the hydrogel matrix and consequently reduces the rate of degradation. In the absence of Pluronic (as in A1) there is a strong crosslinking force due to the amphiphilic interactions between the hydrophilic/hydrophobic portions of the PEG-g-NPHCs copolymer. This also leads to retarding the diffusion of enzyme inside the matrix and consequently reduces the biodegradation rate to an extent similar to or even slightly higher than A2 (10% Pluronic). From the preliminary results obtained and within the range of studied formulations, the micro-particles A2 tend to offer the faster enzymatic degradation.

### **In Vitro Release Studies**

For studying the release profiles, hydrogel micro-particles loaded with SF, as a model for hydrophilic drugs, were prepared by the same procedure used for unloaded microparticles with initial incubation of the drug into the polymers solution prior casting. The estimated EE % of SF in the microparticles were in the range of  $54.06 \pm 2.2$  to  $65.68 \pm 1.1$  (Tab. 1). This reduction in EE% may be attributed to the loss of drug during washing of polymer films prior the cryo-milling. The homogeneous distribution of the uploaded model fluorescein drug SF within the microparticles was confirmed by using fluorescence microscopy as shown in Figure 3.

A comparison between the cumulative release profiles of the hydrogel microparticles A1, A2, and A3 in PBS, pH 7.4, at 37°C in the presence and absence of lysozyme is illustrated in Figure 10. From the figure, three phases were observed during the drug release from the microparticles in the absence and presence of lysozyme; fast initial burst release, which may be due to the high initial swelling attained by the hydrogel microparticles (Figs. 7 and 8), followed by a slow sustained release. In the last phase, a more rapid release was observed which can be attributed to the fast degradation of the microparticles. As shown in Figure 9, in the presence of lysozyme, the biodegradation starts to occur within the first hour. This tends to explain the higher values of drug release attained from the beginning in the presence of lysozyme as compared to lysozyme-free release medium. However, it seems that the micro-particles degradation/dissolution at the third stage occurs faster in the presence of lysozyme leading to more rapid release. These results are in agreement with that observed in the biodegradation study of microparticles (Fig. 9). After 10 days, for instance, the % of SF released from A1, A2, and A3 in the absence of lysozyme were  $30 \pm 0.6\%$ ,  $37 \pm 0.2\%$ , and  $47 \pm 2.6\%$ , respectively. These values were increased to  $97 \pm 2.8\%$ ,  $85 \pm 8.9\%$ , and  $99 \pm 2.5\%$ , respectively, in the presence of lysozyme.

### **Macrophage Uptake Study**

Typically, microparticles are rapidly engulfed and phagocytosed by macrophages in the airways on the order of minutes and this is shown clearly in Figure 11a with nonswellable 1  $\mu$ m polystyrene particles. At 60 min, large amounts of these fluorescent polystyrene microparticles were engulfed (Fig. 11a and Tab. 3). In contrast, swollen hydrogel microparticles, developed in this study (A1 and A3 as examples), had much delayed and reduced macrophage uptake (Tab. 3). This may be attributed to the fast and high swelling attained by these developed microparticles A1 and A3 (see Figs. 7 and 8). Also, the presence of PEG side chains in the PEG-g-Cs copolymer used in the development of these microparticles offers stealth characteristics that help in the macrophage evasion. As shown in Table 3, only at the 12 h time point could phagocytosis of the hydrogels be detected. These preliminary macrophage interaction studies indicate that the swellable hydrogel microparticles designed in these studies may have the potential for sustained release drug delivery to the lung. Current studies are underway to demonstrate the sustained release *in vivo* and evaluate biocompatibility of these delivery systems with therapeutic agents.

## **CONCLUSION**

With this contribution, novel biodegradable physically crosslinked hydrogel microparticles were developed via the amphiphilic interaction between the synthesized PEG-g-Cs copolymer with Pluronic® F-108. The hydrogel microparticles were designed in such a way to display a respirable size (desired aerodynamic size) when dry but attain large swollen size once deposited in lung to avoid the macrophage clearance. The preliminary *in vitro* evaluation of these microparticles showed that they may be tailored to act as potential respirable swellable carriers for pulmonary sustained drug delivery.

## Acknowledgments

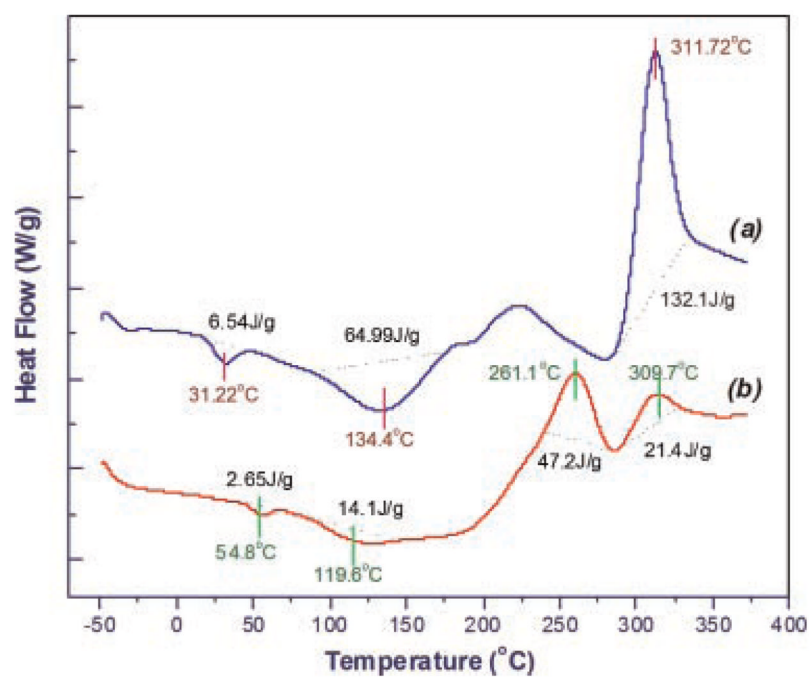
Authors would like to acknowledge the following funding organizations for supporting this work: National Institutes of Health, National Institute of Biomedical Imaging and Bioengineering (REB006892A), PhRMA Foundation, and Oxnard Foundation.

## References

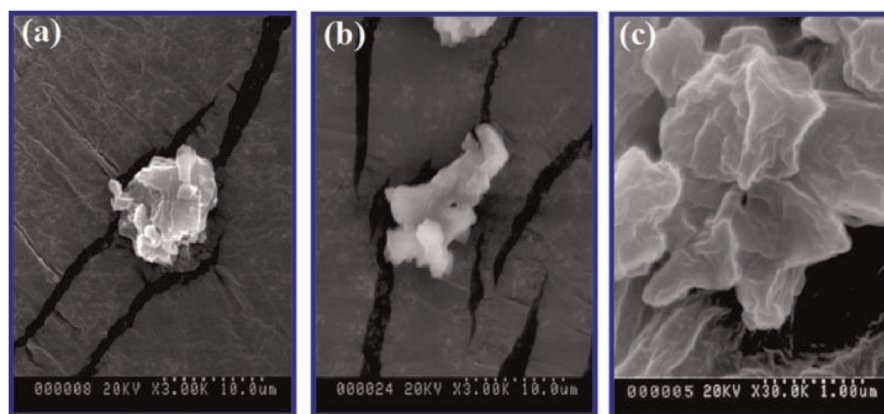
1. Smyth HDC, Garcia-Contreras L. Dry-powder and liquid spray systems for inhaled delivery of peptides and proteins. *Am J Drug Deliv.* 2005; 3:29–45.
2. Courrier HM, Butz N, Vandamme TF. Pulmonary drug delivery systems: Recent developments and prospects. *Crit Rev Ther Drug Carrier Syst.* 2002; 19:425–498. [PubMed: 12661699]
3. Smyth HDC, Hickey AJ. Carriers in drug powder delivery: Implications for inhalation system design. *Am J Drug Deliv.* 2005; 3:117–132.
4. Martonen T, Smyth HDC, Isaccs K, Burton R. Issues in drug delivery: Dry powder inhaler performance and lung deposition. *Respir Care.* 2005; 50:1228–1252. [PubMed: 16163810]
5. Ahsan F, Rivas IP, Khan MA, Suárez-Torres AI. Targeting to macrophages: Role of physicochemical properties of particulate carriers—Liposomes and microspheres on the phagocytosis by macrophages. *J Control Release.* 2002; 79:29–40. [PubMed: 11853916]
6. Makino K, Yamamoto N, Higuchi K, Harada N, Ohshima H, Terada H. Phagocytic uptake of polystyrene micro-spheres by alveolar macrophages: Effects of the size and surface properties of the microspheres. *Colloids Surf B Biointerfaces.* 2003; 27:33–39.
7. Hirano, S.; Seino, H.; Akiyama, Y.; Nonaka, I. Chitosan: A biocompatible material for oral and intravenous administration. In: Gebelin, CG.; Dunn, RL., editors. *Progress in biomedical polymers.* New York: Plenum Press; 1990. p. 283-298.
8. Xie WM, Xu PX, Wang W, Liu Q. Preparation and antibacterial activity of a water-soluble chitosan derivative. *Carbohydr Polym.* 2002; 50:35–40.
9. Wang PF, Wu SHK, Shi XY, Deng BM, Sun C. The aggregation behavior of chitosan bioelectret in aqueous solution using a fluorescence probe. *J Mater Sci.* 1998; 33:1753–1757.
10. Kim C, Lee SC, Kang SW, Kwon IC, Kim YH, Jeong SY. Synthesis and the micellar characteristics of poly(ethylene oxide)-deoxycholic acid conjugates. *Langmuir.* 2000; 16:4792–4797.
11. Huh KM, Lee KY, Kwon IC, Kim YH, Kim C, Jeong SY. Synthesis of triarmed poly(ethylene oxide)-deoxycholic acid conjugate and its micellar characteristics. *Langmuir.* 2000; 16:10566–10568.
12. Nishikawa T, Akiyoshi K, Sunamoto J. Macromolecular complexation between bovine serum albumin and the self-assembled hydrogel nanoparticle of hydrophobized polysaccharides. *J Am Chem Soc.* 1996; 118:6110–6115.
13. Nichifor M, Lopes A, Carpoy A, Melo E. Aggregation in water of dextran hydrophobically modified with bile acids. *Macromolecules.* 1999; 32:7078–7085.
14. Na K, Lee ES, Bae YH. Adriamycin loaded pullulan acetate/sulfonamide conjugate nanoparticles responding to tumor pH: pH-dependent cell interaction, internalization and cytotoxicity in vitro. *J Control Release.* 2003; 87:3–13. [PubMed: 12618018]
15. Parka JH, Kwona S, Lee M, Chunga H, Kim JH, Kimc YS, Park RW, Kim IS, Seod SB, Kwona IC, Jeong SY. Self-assembled nanoparticles based on glycol chitosan bearing hydrophobic moieties as carriers for doxorubicin: In vivo bio-distribution and anti-tumor activity. *Biomaterials.* 2006; 27:119–126. [PubMed: 16023198]
16. Dufes C, Schatzlein AG, Tetley L, Gray AI, Watson DG, Olivier JC, Couet W, Uchegbu IF. Niosomes and polymeric chitosan based vesicles bearing transferring and glucose ligands for drug targeting. *Pharm Res.* 2000; 17:1250–1258. [PubMed: 11145231]
17. El-Sherbiny IM, Lins RJ, Abdel-Bary EM, Harding DRK. Preparation, characterization, swelling and in vitro drug release behaviour of poly[N-acryloylglycinechitosan] interpolymeric pH and thermally-responsive hydrogels. *Eur Polym J.* 2005; 41:2584–2591.

18. El-Sherbiny IM, Abdel-Bary EM, Harding DRK. Swelling characteristics and in vitro drug release study with pH- and thermally sensitive hydrogels based on modified chitosan. *J Appl Polym Sci.* 2006; 102:977–985.
19. Ohya Y, Cai R, Nishizawa H, Hara K, Ouchi T. Preparation of PEG-grafted chitosan nanoparticles as peptide drug carriers. *STP Pharm Sci.* 2000; 10:77–82.
20. Zhang X, Zhang H, Wu Z, Wang Z, Niu H, Li C. Nasal absorption enhancement of insulin using PEG-grafted chitosan nanoparticles. *Eur J Pharm Biopharm.* 2008; 68:526–534. [PubMed: 17881202]
21. Prego C, Torres D, Fernandez-Megia E, Novoa-Carballal R, Quiñoá E, Alonso MJ. Chitosan–PEG nanocapsules as new carriers for oral peptide delivery: Effect of chitosan pegylation degree. *J Control Release.* 2006; 111:299–308. [PubMed: 16481062]
22. Yao Z, Zhang C, Ping Q, Yu L. A series of novel chitosan derivatives: Synthesis, characterization and micellar solubilization of paclitaxel. *Carbohydr Polym.* 2007; 68:781–792.
23. Mao S, Shuaia X, Ungera F, Wittmara M, Xiec X, Kissel T. Synthesis, characterization and cytotoxicity of poly (ethylene glycol)-graft-trimethyl chitosan block copolymers. *Biomaterials.* 2005; 26:6343–6356. [PubMed: 15913769]
24. Opanasopit P, Ngawhirunpat T, Rojanarata T, Choochottiros C, Chirachanchai S. N-phthaloyl chitosan-g-mPEG design for all-trans retinoic acid-loaded polymeric micelles. *Eur J Pharm Sci.* 2007; 30:424–431. [PubMed: 17307343]
25. Zhang XG, Teng DY, Wu ZM, Wang X, Wang Z, Yu DM, Li CX. PEG-grafted chitosan nanoparticles as an injectable carrier for sustained protein release. *J Mater Sci.* 2008; 19:3525–3533.
26. Opanasopit P, Ngawhirunpat T, Chaidegumjorn A, Rojanarata T, Apirakaramwong A, Phongying S, Choochottiros C, Chirachanchai S. Incorporation of camptothecin into N-phthaloyl chitosan-g-mPEG self-assembly micellar system. *Eur J Pharm Biopharm.* 2006; 64:269–276. [PubMed: 16870407]
27. Batrakova EV, Kabanov AV. Pluronic block copolymers: Evolution of drug delivery concept from inert nanocarriers to biological response modifiers. *J Control Release.* 2008; 130:98–106. [PubMed: 18534704]
28. Terada S, Yoshimoto H, Fuchs JR, Sato M, Pomerantseva I, Selig MK, Hannouche D, Vaccanti JP. Hydrogel optimization for cultured elastic chondrocytes seeded onto a polyglycolic acid scaffold. *J Biomed Mater Res.* 2005; 75A:907–916.
29. Wesenberg-Ward KE, Tyler BJ, Sears JT. Adhesion and biofilm formation of *Candida albicans* on native and pluronic-treated polystyrene. *Biofilms.* 2005; 2:63–71.
30. England JL. Stabilization and release effects of Pluronic® F127 in protein drug delivery. *JUS.* 1999; 5:17–24.
31. Grassi G, Farra R, Caliceti P, Guarnieri G, Salmaso S, Carenza M, Grassi M. Temperature-sensitive hydrogels: Potential therapeutic applications. *Am J Drug Deliv.* 2005; 3:239–251.
32. Yoksan R, Matsusaki M, Akashi M, Chirachanchai S. Controlled hydrophobic/hydrophilic chitosan: Colloidal phenomena and nanosphere formation. *Colloid Polym Sci.* 2004; 282:337–342.
33. Yoksan R, Chirachanchai S. Amphiphilic chitosan nanosphere: Studies on formation, toxicity, and guest molecule incorporation. *Bioorg Med Chem.* 2008; 16:2687–2696. [PubMed: 18061462]
34. Nsereko S, Amiji M. Localized delivery of paclitaxel in solid tumors from biodegradable chitin microparticle formulations. *Biomaterials.* 2002; 23:2723–2731. [PubMed: 12059022]
35. Hirano S, Tsuchida H, Nagao N. N-acetylation in chitosan and the rate of its enzymic hydrolysis. *Biomaterials.* 1989; 10:574–576. [PubMed: 2605289]
36. Sharma R, Muttill P, Yadav AB, Rath SK, Bajpai VK, Mani U, Misra A. Uptake of inhalable microparticles affects defence responses of macrophages infected with *Mycobacterium tuberculosis* H37Ra. *J Antimicrob Chemother.* 2007; 59:499–506. [PubMed: 17242031]
37. Guinesi LS, Cavalheiro ETG. The use of DSC curves to determine the acetylation degree of chitin/chitosan samples. *Thermochim Acta.* 2006; 444:128–133.
38. Kittur FS, Prashanth KVH, Sankar KU, Tharanthan RN. Characterization of chitin, chitosan and their carboxymethyl derivatives by differential scanning calorimetry. *Carbohydr Polym.* 2002; 49:185–193.

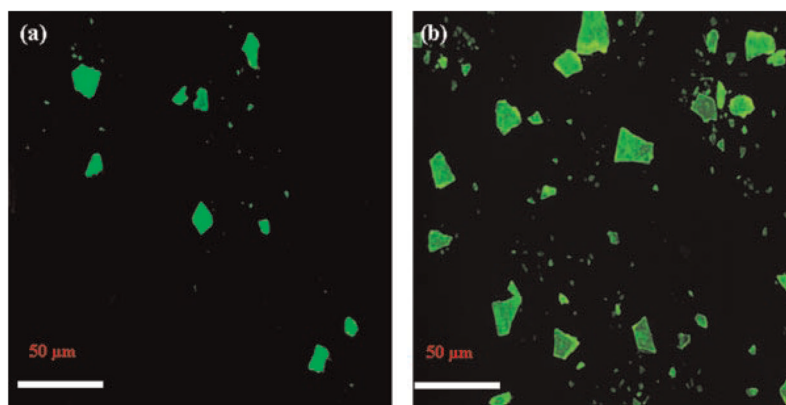
39. Ortega-Rivas, E. Handling and processing of food powders and particulates. In: Onwulata, C., editor. Encapsulated and powdered foods. Boca Raton: CRC Press, Taylor & Francis G; 2005. p. 78-81.
40. Chrystyn H. The Diskus<sup>TM</sup>: A review of its position among dry powder inhaler devices. *Int J Clin Pract.* 2007; 61:1022–1036. [PubMed: 17504364]
41. Hinds, WC. Uniform particle motion. In: Hinds, WC., editor. *Aerosol technology: Properties, behavior and measurement of airborne particles*. New York: John Wiley & Sons, Inc; 1999. p. 42-74.



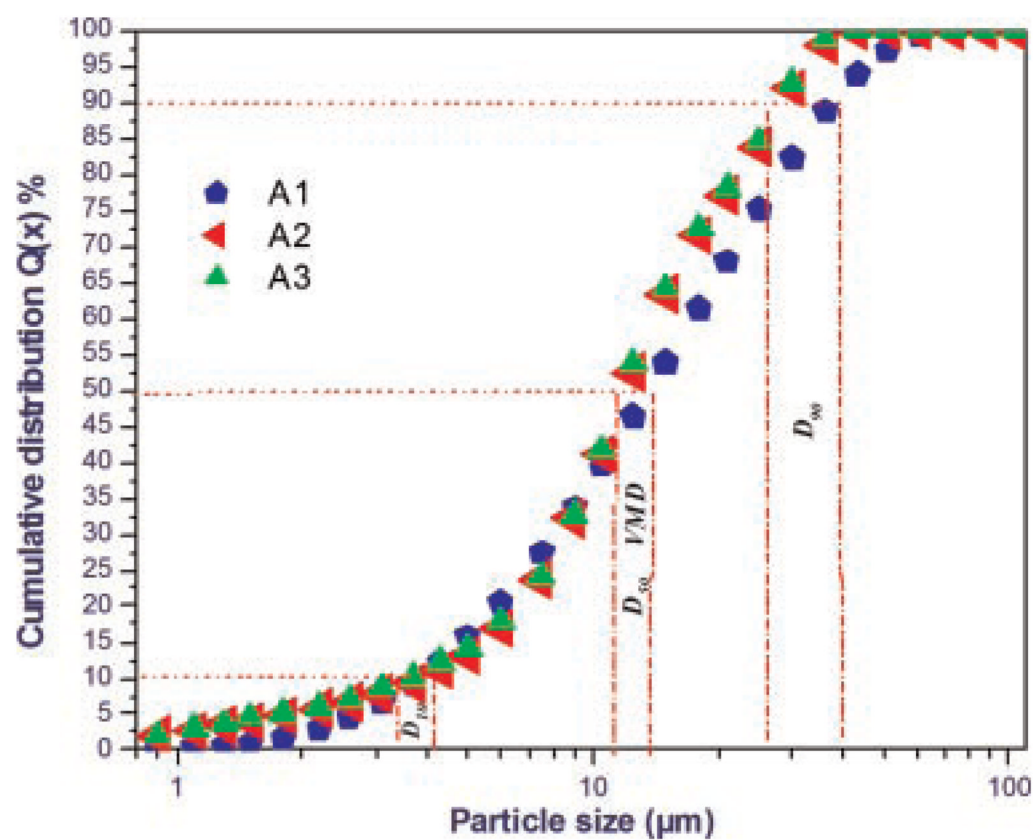
**Figure 1.**  
DSC of the synthesized PEG-g-Cs copolymer in comparison with Cs.



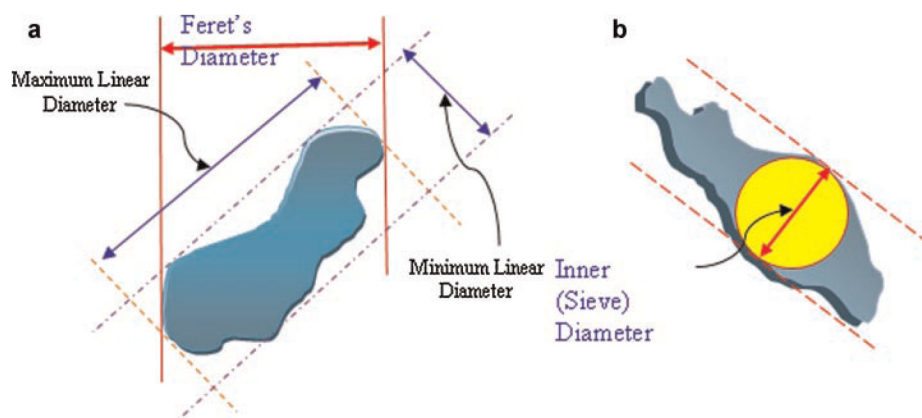
**Figure 2.** Scanning electron micrographs of (a) A1, (b) A3, and (c) surface of SF-loaded A1 microparticles.



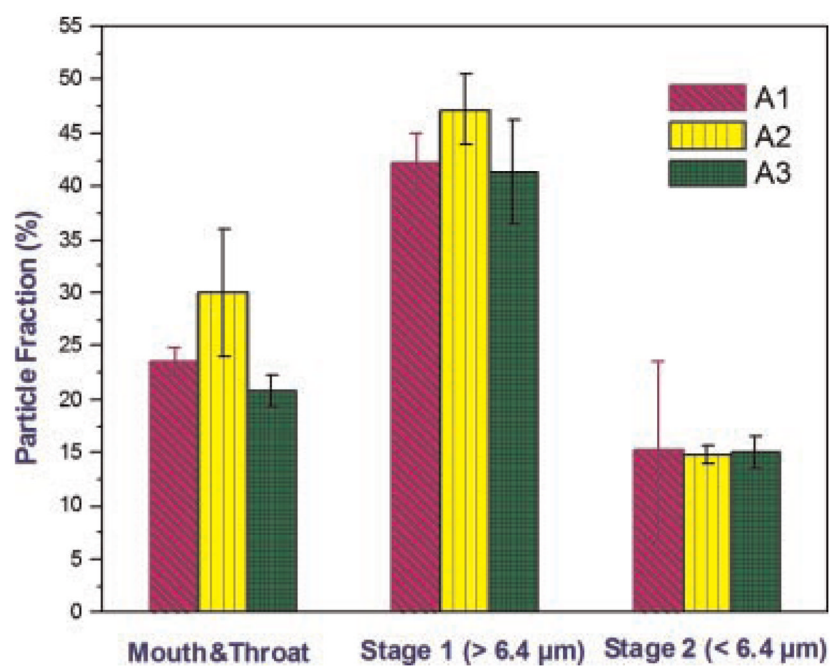
**Figure 3.** Microscopic images illustrating the differences in size and SF distribution of some dry SF-loaded (a) PEG-g-CS (A1) and (b) PEG-g-CS/Pluronic® (A3) hydrogel microparticles.



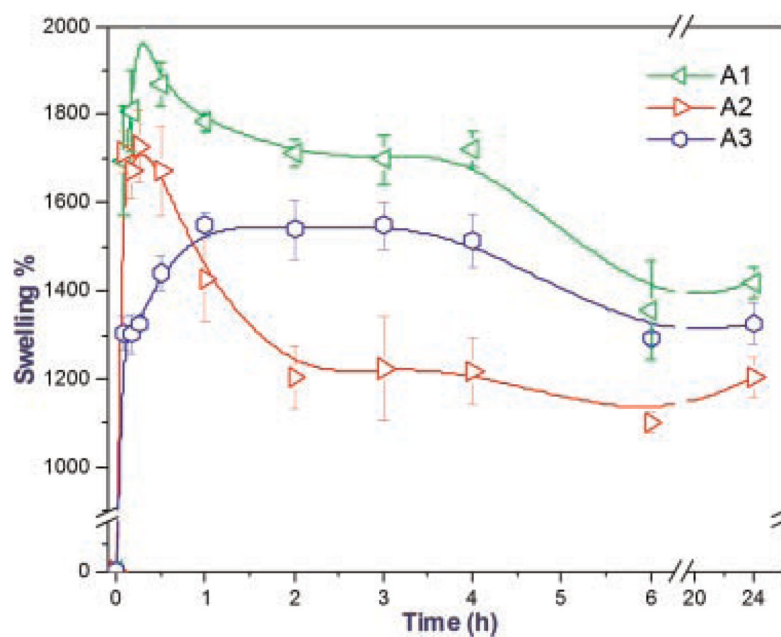
**Figure 4.**  
The cumulative size distribution of the developed microparticles as determined by laser diffraction.



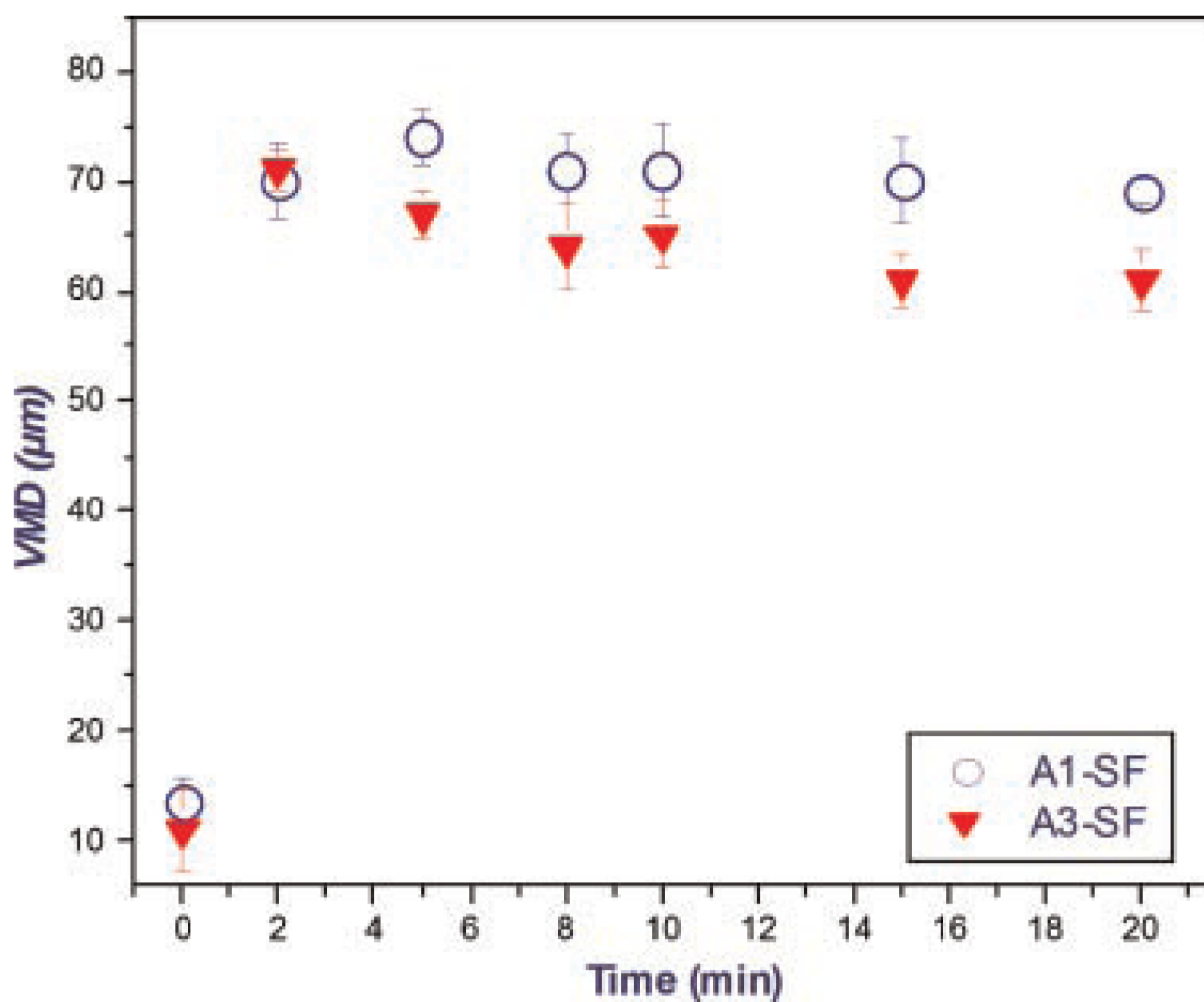
**Figure 5.**  
A schematic illustration of (a) Feret's and (b) inner (Sieve) diameters of irregular particles.



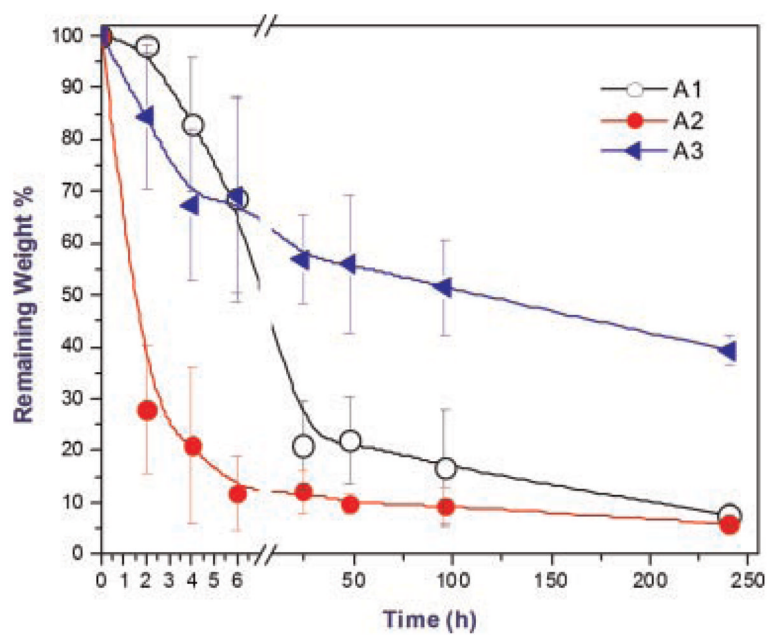
**Figure 6.**  
Aerodynamic evaluation of the microparticles A1–A3 using a twin-stage impinger (TSI) with the aerolizer inhaler.



**Figure 7.** Swelling patterns of the SF-loaded hydrogel microparticles in PBS (pH 7.4) at 37°C (mean  $\pm$  SD,  $n=3$ ).

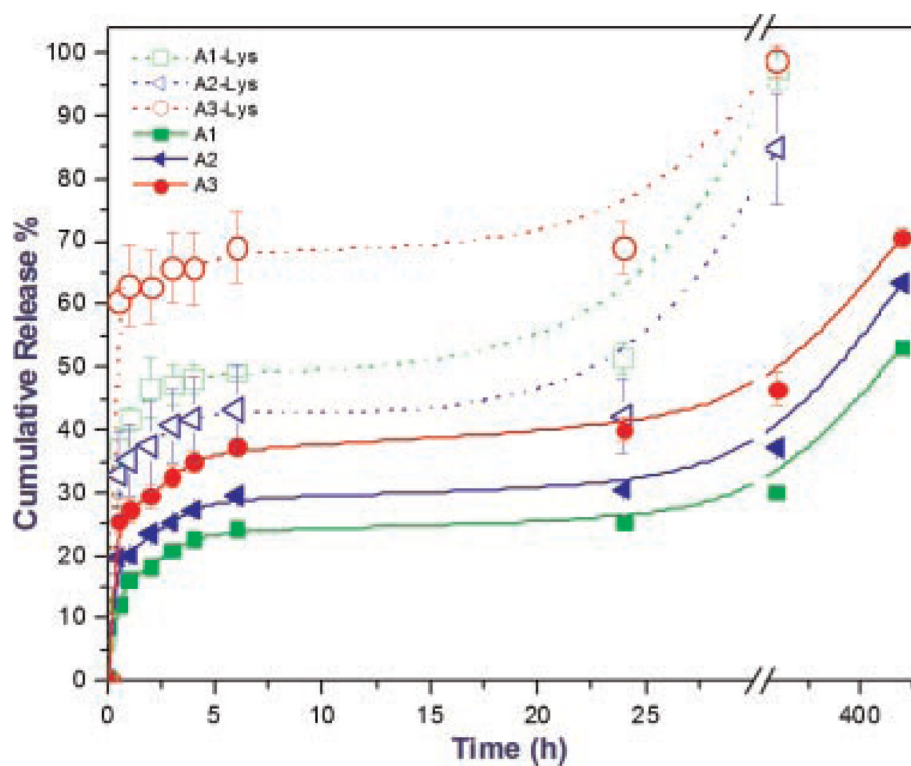


**Figure 8.**  
Volume median diameter (VMD,  $\mu\text{m}$ ) of swelled SF-loaded A1 and A3 microparticles.



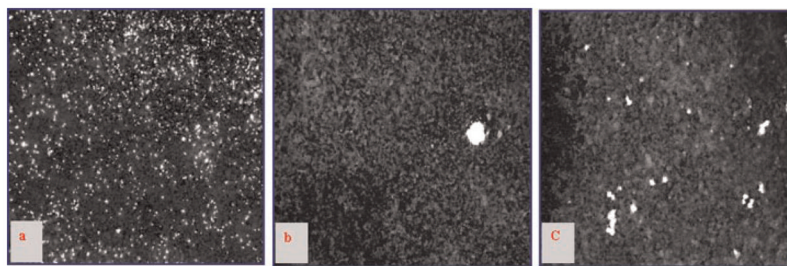
**Figure 9.**

The enzymatic degradation profiles of the prepared hydrogel microparticles in phosphate buffer (PBS, pH 7.4) in the presence of lysozyme (mean  $\pm$  SD,  $n = 3$ ).



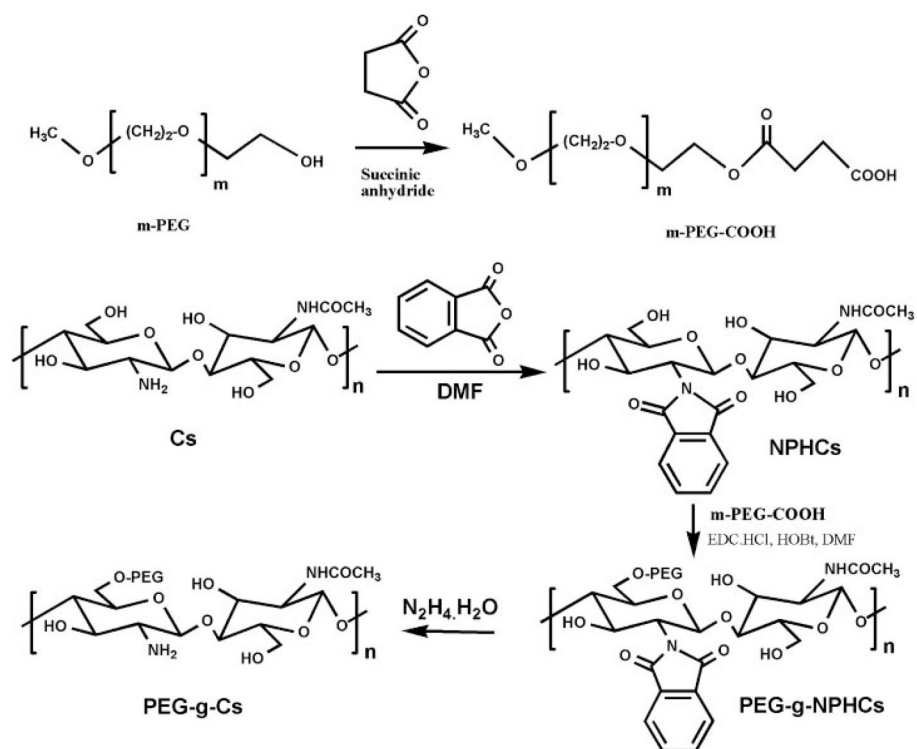
**Figure 10.**

Comparison between the cumulative release profiles of the hydrogel microparticles: A1, A2, and A3 in PBS, pH 7.4, at 37°C in the presence and absence of lysozyme.

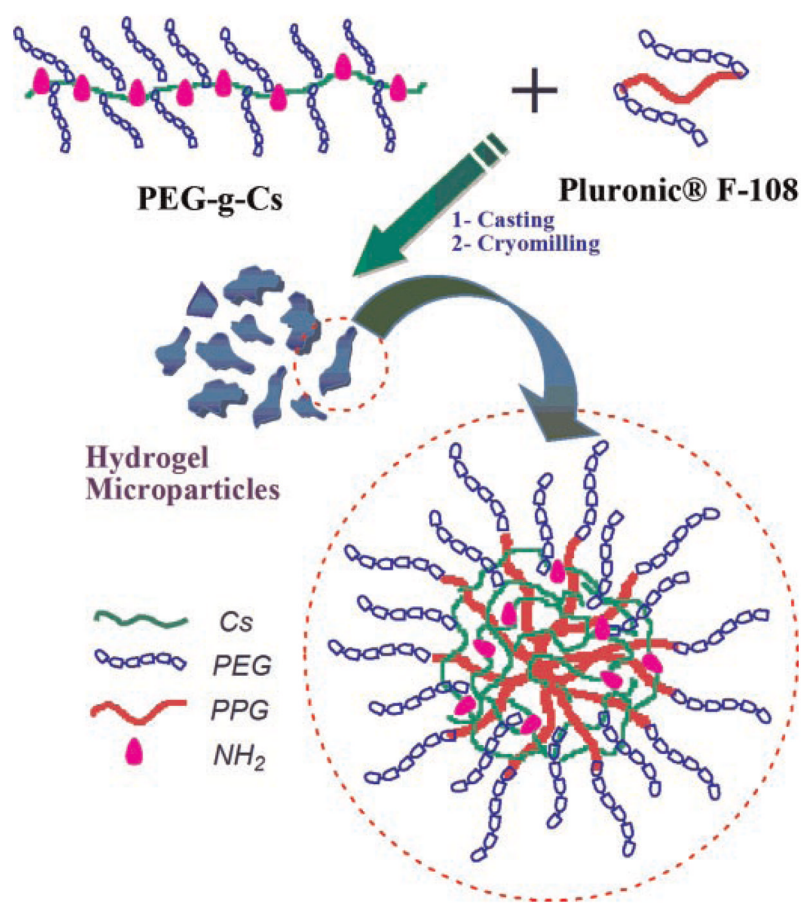


**Figure 11.**

Particle uptake by macrophages *in vitro*: (a) nonswellable 1  $\mu\text{m}$  beads at 60 min incubation time point, (b) swellable A1 particle at 12 h, and (c) swellable A3 particles at 12 h. Fluorescent imaging of retained particles was determined at wide field low magnification (4 $\times$ ).

**Scheme 1.**

Schematic illustration of the synthesis of PEG-g-Cs copolymer.

**Scheme 2.**

Schematic representation of the developed hydrogel microparticles.

**Table 1**

Composition of the Developed Hydrogel Microparticles, Their Drug Entrapment Efficiencies, and Moisture Contents

Sample Code	PEG-g-Cs		Pluronic® F-108		Moisture Content (%)	
	W%	Vol <sup>a</sup> (mL)	W%	Vol <sup>a</sup> (mL)	EE% ± SD	Plain
A1	100	50	—	—	54.06 ± 2.22	0.41 ± 0.06
A2	90	45	10	5	65.68 ± 1.09	0.27 ± 0.00
A3	60	30	40	20	55.38 ± 2.63	0.27 ± 0.00

EE%; entrapment efficiency (%).

<sup>a</sup>The concentration of polymer solutions used was 1% (w/w).

**Table 2**

Geometric Diameters, Aerodynamic Characteristics, and Tapped (Bulk) Density of the Developed Hydrogel Microparticles

Sample Code	Mean Diameter ( $\mu\text{m}$ )		VMD, $D_{50}$ ( $\mu\text{m}$ )	Span <sup>a</sup>	Mean Area <sup>b</sup> ( $\mu\text{m}^2$ )	Powder Wt. <sup>c</sup> (mg)	EF (%)	TSI-RF (%)	Bulk Density ( $\text{g}/\text{cm}^3$ )	
	Feret's	Sieve							Plain	SF-Loaded
A1	21.81	12.78	13.73 $\pm$ 0.07	2.44 $\pm$ 0.02	207.19	85.0	98 $\pm$ 0.9	15.24 $\pm$ 8.46	0.704	0.788
A2	17.10	10.96	12.06 $\pm$ 0.13	2.05 $\pm$ 0.02	160.47	75.7	96 $\pm$ 2.1	14.85 $\pm$ 0.87	0.718	0.746
A3	16.67	11.83	11.13 $\pm$ 0.23	2.18 $\pm$ 0.09	156.98	74.3	96 $\pm$ 1.8	15.07 $\pm$ 0.58	0.723	0.706

VMD, volume median diameter; EF, emitted fraction; RF, respirable fraction.

<sup>a</sup>Span =  $(D_{90} - D_{10})/D_{50}$  (see Fig. 2).

<sup>b</sup>Mean area as estimated using ImageJ software ( $n = 100$ ).

<sup>c</sup>Total wt. of powder loaded in three capsules.

**Table 3**

The Number of Microparticles Taken Up by Macrophages In Vitro for Nonswellable and Swellable Particles as a Function of Time

Time	Nonswellable Particles	Swellable A1	Swellable A3
15 min	417	0	0
30 min	627	0	0
60 min	2686	0	0
12 h	14,428	1	35
24 h	CNBD	3	8

CNBD, could not be determined due to inability to distinguish individual particles at high particle numbers.